Focusing of surface phonon polaritons

A. J. Huber,[1,2] B. Deutsch,[3] L. Novotny,[3] and R. Hillenbrand[1,2,a)]
[1]*Nano-Photonics Group, Max-Planck-Institut für Biochemie, D-82152 Martinsried, Germany*
[2]*Nanooptics Laboratory, CIC NanoGUNE Consolider, P. Mikeletegi 56, 20009 Donostia-San Sebastián, Spain*
[3]*The Institute of Optics, University of Rochester, Rochester, New York 14611, USA*

(Received 17 March 2008; accepted 24 April 2008; published online 20 May 2008)

Surface phonon polaritons (SPs) on crystal substrates have applications in microscopy, biosensing, and photonics. Here, we demonstrate focusing of SPs on a silicon carbide (SiC) crystal. A simple metal-film element is fabricated on the SiC sample in order to focus the surface waves. Pseudoheterodyne scanning near-field infrared microscopy is used to obtain amplitude and phase maps of the local fields verifying the enhanced amplitude in the focus. Simulations of this system are presented, based on a modified Huygens' principle, which show good agreement with the experimental results. © *2008 American Institute of Physics*. [DOI: 10.1063/1.2930681]

Surface phonon polaritons (SPs) are electromagnetic surface modes formed by the strong coupling of light and optical phonons in polar crystals, and are generally excited using infrared (IR) or terahertz (THz) radiation.[1] Generation and control of surface phonon polaritons are essential for realizing novel applications in microscopy,[2,3] data storage,[4] thermal emission,[2,5] or in the field of metamaterials.[6] Materials supporting SPs such as SiC, quartz, or GaN offer strong temperature stability, anisotropic properties, and also the ability to strongly couple phonon and plasmon polaritons by doping,[7,8] which could be exploited in photonic applications.

Controlling, guiding, and focusing surface polaritons by optical elements has been recently shown with surface *plasmon* polaritons at visible and near-infrared wavelengths,[9–17] but comparatively little attention has been given to surface *phonon* polaritons despite certain advantages including their ability to be generated in a wide spectral range, from IR to terahertz wavelengths (typically between 8 and 200 μm) at the surface of a large variety of semiconductors, insulators, and ferroelectrics. In this paper, we experimentally realize focused SPs at mid-IR frequencies, and use scattering-type scanning near-field optical microscopy[18,19] (s-SNOM) with pseudoheterodyne detection[20] to map spatially the surface polaritons with subwavelength resolution in amplitude and phase. Focusing of SPs could be essential for applications that require localized IR or terahertz fields including photodetectors and emitters.

Polariton propagation on a material's surface requires a negative dielectric constant, which may result from collective conduction electron oscillations (plasmon polaritons)[11,14,21,22] or from lattice vibrations in polar crystals (phonon polaritons).[1,23,24] For SPs, the electric field E_p is strongly coupled to lattice vibrations and is confined to surface propagation with the electromagnetic energy density falling off evanescently with distance from the surface.[1] The exponential decay of E_p perpendicular to the surface (z direction) is given by $E_p \sim e^{-k_{p,z}z}$ with

$$k_{p,z} = \left[k_{p,x}^2 - \left(\frac{\omega}{c} \right)^2 \right]^{1/2}. \tag{1}$$

For the 4*H*-SiC crystal used in our experiments, the SP propagation in x direction is described by the complex-valued wave vector (dispersion relation)

$$k_{p,x} = k'_{p,x} + ik''_{p,x} = \frac{\omega}{c} \sqrt{\frac{\varepsilon_\parallel \varepsilon_\perp - \varepsilon_\perp}{\varepsilon_\parallel \varepsilon_\perp - 1}}. \tag{2}$$

Here, $\varepsilon_\parallel$ and $\varepsilon_\perp$ are the complex-valued dielectric constants parallel and perpendicular to the c-axis of the crystal, respectively, ω is the angular frequency, and c the speed of light. Optical energy can be coupled into surface polariton modes at discontinuities in the material.[14,25] In our experiment, we apply the edge-coupling method to excite SPs on a 4*H*-SiC crystal.[26,27]

Figure 1 is a schematic illustration of our experimental setup. The element used for surface phonon polariton excitation and focusing is a ring-shaped, 25 nm thick Au film which was fabricated by conventional optical lithography on the SiC crystal. The width of the element is 20 μm and the opening angle is 90°. In our experimental configuration, both the element and the probing tip of the s-SNOM are illuminated with angle $\alpha \approx 45°$ relative to the sample surface. The s-SNOM used in this experiment has been described in detail

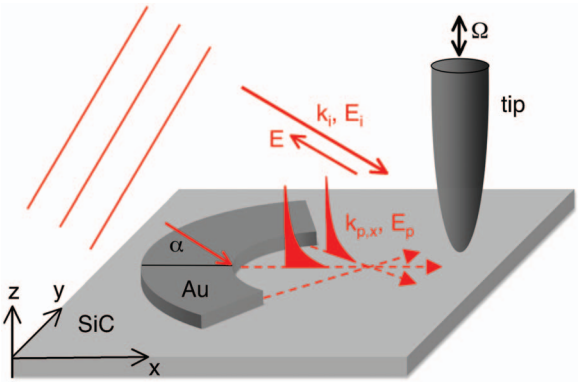

FIG. 1. (Color) Experimental setup for demonstrating SP focusing. A circular Au structure excites and focuses surface phonon polaritons on a SiC crystal when illuminated by a plane wave with $\lambda = 10.85$ μm. The tip of a scattering-type near-field optical microscope scans the sample surface in order to map the local field.

a)Electronic mail: hillenbr@biochem.mpg.de.

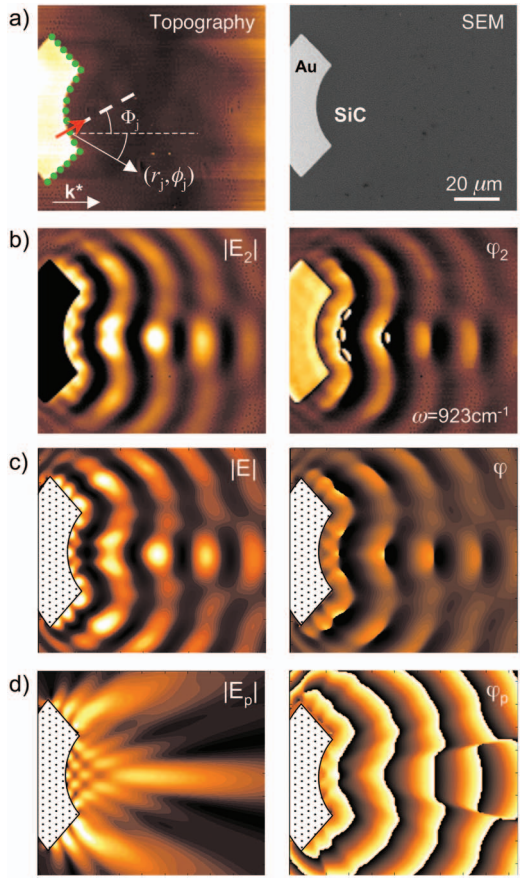

FIG. 2. (Color) (a) AFM topography (left) and scanning electron microscopy image (SEM, right) of the focusing element (Au) on the SiC surface. The in-plane projection of the illuminating wave vector (k^*) is shown by a white arrow in the topography image. Dipole emitters used for our simulations [(c) and (d)] are schematically represented by green points, and the red arrow represents the orientation (Φ_j) of the jth dipole emitter. (b) IR s-SNOM images showing amplitude $|E_2|$ (left) and φ_2. (c) Simulations of the local field E showing amplitude $|E|$ (left) and phase φ (right). (d) Simulations of the surface phonon polariton field E_p showing amplitude $|E_p|$ (left) and phase φ_p (right) without the illuminating field.

in previous works.[18,26] It is based on a tapping-mode atomic force microscope (AFM) where the tip vibrates at the cantilever resonance frequency Ω. Infrared laser light from a tuneable CO_2 laser is focused on the tip-sample region and a Michelson interferometer is used to collect the backscattered light. In order to form an image, the sample is raster scanned. It has been shown previously that demodulating the detected signal at higher harmonics $n\Omega$ of the cantilever resonance frequency Ω has the effect of suppressing background signals caused by scattering from the sample and tip shaft.[18] Pseudoheterodyne[20] interferometric detection yields amplitude $|E_2|$ and phase φ_2 signals by demodulating the detector output with $n=2$.

In s-SNOM, the demodulated interferometric signal is, in general, nontrivially related to the amplitude $|E|$ and phase φ of the local field E illuminating the tip apex, $E=|E|e^{i\varphi}$. However, it has been shown that for surface phonon polaritons on SiC, the measured amplitude $|E_2|$ and phase φ_2 signals are given by $|E_2| \propto |E|$ and $\varphi_2=\varphi$.[26] The local field $E=E_i+E_p$ is the sum of the illuminating field E_i and the surface phonon polariton field E_p at the position of the tip apex.

Figure 2(b) shows the amplitude $|E_2|$ and phase φ_2 images of the area around the focusing element irradiated with light of the wavelength $\lambda=10.85$ μm. The optical images show fringes due to the interference between the incident field E_i and the SP field E_p.[26,27] At about 40 μm distance from the focusing element, we clearly observe SP localization in the y direction with an enhanced amplitude signal $|E_2|$, providing evidence of a surface phonon polariton focus. We note that at $\lambda=10.85$ μm the propagation length of the phonon polariton is approximately 60 μm.[26,27]

For describing the s-SNOM images theoretically, we perform a mathematical simulation (Figs. 2(c) and 2(d)) by using a simple model based on the Huygens principle. We model the SP field as originating from an array of 120 point emitters along the Au edge. Note that the simulation results do not change appreciably upon increasing the number of point emitters. In contrast to the Huygens principle in far-field optics, however, we need to replace the isotropic emitter by a point dipole emitter with polarization parallel to the surface.[9,10,13,16,28] For best agreement with the experiment, we furthermore find that each dipole must be oriented normal to the Au edge. Interestingly, the dipole orientation is then not necessarily parallel to the projected wave vector of the incident light in the plane of the sample k^*. A related observation has been recently reported with surface plasmon polaritons focused by a circular nanoparticle chain.[16] In our simulation, the jth dipole launching a SP is excited by the illuminating field with a phase lag proportional to its distance from the tip in the x direction. Thus, the surface phonon polariton field resulting from the jth dipole observed at (r_j, ϕ_j) is given in polar coordinates by

$$E_{p,j} = \frac{|E_i| f_0}{\sqrt{r_j}} e^{i(k_{p,x} r_j - k r_j \cos\alpha \cos\phi_j + \phi_0)} \cos\Phi_j, \tag{3}$$

where ϕ_0 is a constant phase offset and f_0 the relative field amplitude. E_p is the sum of the fields of these dipole emitters, and the total field at the tip is given by

$$E = E_i + E_p = |E_i| \left[1 + \sum_{j=0}^{n} \frac{f_0}{\sqrt{r_j}} e^{i(k_{p,x} r_j - k r_j \cos\alpha \cos\phi_j + \phi_0)} \cos\Phi_j \right]. \tag{4}$$

Using Eq. (4), simulations of the s-SNOM images were performed, and the results are shown in Fig. 2(c). The value of $k_{p,x}$ was obtained from Eq. (2) and two free parameters, the relative amplitude $f_0=2.4$ and the constant phase $\phi_0=135°$ were adjusted to match the experimental s-SNOM data. The results for $|E|$ and φ are in excellent agreement with the experimental images $|E_2|$ and φ_2, respectively, indicating that the model in Eq. (4) is satisfactory to describe surface phonon polariton propagation on structured SiC surfaces. Even fine details such as the SP interference near the Au structure are clearly reproduced.

In Fig. 2(d), we present the simulated SP field E_p only, showing more clearly the focal field. In the amplitude image $|E_p|$, we find that the focus is shifted away from the center of the element's radius of curvature. This is a result of the oblique illumination and has been recently demonstrated with surface plasmon polaritons.[15] The calculated phase image φ_p shows the phase evolution cycling through 2π, as expected for propagating SPs. Comparing the simulated phase fronts and the experimental images provides evidence that the fringes observed by our experimental configuration directly visualize the evolution of the SP wavefronts. Between element and focal region, they appear to converge, and after the

focus, to diverge. Our method of SP imaging could thus find interesting application in studying the wavefront evolution of surface phonon polaritons on structured crystal surfaces as well as of surface plasmon polaritons on structured metal films[29,30] and metamaterials.

In conclusion, surface phonon polaritons receive less attention than surface plasmon polaritons, even though their properties make them attractive for applications in microscopy, photonics and sensorics in the IR to terahertz spectral regime. For future applications, control techniques for surface phonon polaritons must be developed. Here, we have demonstrated that surface phonon polaritons can be focused using simple elements. This is an encouraging result, and should aid in the use of surface phonon polaritons in their promising applications.

The authors would like to acknowledge M. Hoeb (TU Munich) for the help with optical lithography and N. Ocelic (MPI) for stimulating discussions. Supported by BMBF Grant No. 03N9705, and the Air Force Office of Scientific Research (F-49620-03-1-0379, MURI).

[1] G. Borstel and H. Falge, in *Electromagnetic Surface Modes*, edited by A. D. Boardman (Wiley, Chichester, 1982), p. 221.
[2] Y. De Wilde, F. Formanek, R. Carminati, B. Gralak, P. A. Lemoine, K. Joulain, J. P. Mulet, Y. Chen, and J. J. Greffet, Nature (London) **444**, 740 (2006).
[3] T. Taubner, D. Korobkin, Y. Urzhumov, G. Shvets, and R. Hillenbrand, Science **313**, 1595 (2006).
[4] N. Ocelic and R. Hillenbrand, Nat. Mater. **3**, 606 (2004).
[5] J. J. Greffet, R. Carminati, K. Joulain, J. P. Mulet, S. P. Mainguy, and Y. Chen, Nature (London) **416**, 61 (2002).
[6] D. Korobkin, Y. A. Urzhumov, B. Neuner, C. Zorman, Z. Zhang, I. D. Mayergoyz, and G. Shvets, Appl. Phys. A: Mater. Sci. Process. **88**, 605 (2007).
[7] R. Hillenbrand, Ultramicroscopy **100**, 421 (2004).
[8] T. Taubner, F. Keilmann, and R. Hillenbrand, Nano Lett. **4**, 1669 (2004).
[9] A. Bouhelier, T. Huser, H. Tamaru, H. J. Guntherodt, D. W. Pohl, F. I. Baida, and D. Van Labeke, Phys. Rev. B **63**, 155404 (2001).
[10] H. Ditlbacher, J. R. Krenn, G. Schider, A. Leitner, and F. R. Aussenegg, Appl. Phys. Lett. **81**, 1762 (2002).
[11] W. L. Barnes, A. Dereux, and T. W. Ebbesen, Nature (London) **424**, 824 (2003).
[12] J. R. Krenn and J. C. Weeber, Philos. Trans. R. Soc. London, Ser. A **362**, 739 (2004).
[13] L. Yin, V. K. Vlasko-Vlasov, J. Pearson, J. M. Hiller, J. Hua, U. Welp, D. E. Brown, and C. W. Kimball, Nano Lett. **5**, 1399 (2005).
[14] A. V. Zayats, I. I. Smolyaninov, and A. Maradudin, Phys. Rep., Phys. Lett. **408**, 131 (2005).
[15] Z. Liu, J. M. Steele, H. Lee, and X. Zhang, Appl. Phys. Lett. **88**, 171108 (2006).
[16] A. B. Evlyukhin, S. I. Bozhevolnyi, A. L. Stepanov, R. Kiyan, C. Reinhardt, S. Passinger, and B. N. Chichkov, Opt. Express **15**, 16667 (2007).
[17] S. Maier, *Plasmonics: Fundamentals and Applications* (Springer, Berlin, 2007).
[18] F. Keilmann and R. Hillenbrand, Philos. Trans. R. Soc. London, Ser. A **362**, 787 (2004).
[19] B. Deutsch, R. Hillenbrand, and L. Novotny, Opt. Express **16**, 494 (2008).
[20] N. Ocelic, A. Huber, and R. Hillenbrand, Appl. Phys. Lett. **89**, 101124 (2006).
[21] H. Räther, *Surface Plasmons* (Springer, Berlin, 1988).
[22] L. Novotny and B. Hecht, *Principles of Nano Optics* (Cambridge Universtiy Press, Cambridge, 2006).
[23] R. Ruppin and R. Englman, Rep. Prog. Phys. **33**, 149 (1970).
[24] D. L. Mills and E. Burstein, Rep. Prog. Phys. **37**, 817 (1974).
[25] L. Salomon, G. Bassou, H. Aourag, J. P. Dufour, F. de Fornel, F. Carcenac, and A. V. Zayats, Phys. Rev. B **65**, 125409 (2002).
[26] A. Huber, N. Ocelic, D. Kazantsev, and R. Hillenbrand, Appl. Phys. Lett. **87**, 081103 (2005).
[27] A. J. Huber, N. Ocelic, and R. Hillenbrand, J. Microsc. **229**, 389 (2008).
[28] F. I. Baida, D. Van Labeke, A. Bouhelier, T. Huser, and D. W. Pohl, J. Opt. Soc. Am. A Opt. Image Sci. Vis **18**, 1552 (2001).
[29] T. Rindzevicius, Y. Alaverdyan, B. Sepulveda, T. Pakizeh, M. Kall, R. Hillenbrand, J. Aizpurua, and F. J. G. de Abajo, J. Phys. Chem. C **111**, 1207 (2007).
[30] Y. C. Chang, J. Y. Chu, T. J. Wang, M. W. Lin, J. T. Yeh, and J. K. Wang, Opt. Express **16**, 740 (2008).